LWT - Food Science and Technology 79 (2017) 428–436

Contents lists available at ScienceDirect

LWT - Food Science and Technology

journal homepage: www.elsevier.com/locate/lwt

Evaluation of the metabolic response of *Escherichia coli* to electrolysed water by ^{1}H NMR spectroscopy

Qin Liu [a, c], Ji'en Wu [b], Zhi Yang Lim [a], Arushi Aggarwal [c, 1], Hongshun Yang [a, c, *], Shifei Wang [d]

[a] Food Science and Technology Programme, c/o Department of Chemistry, National University of Singapore, Singapore 117543, Singapore
[b] The Nuclear Magnetic Resonance Laboratory, Department of Chemistry, National University of Singapore, 3 Science Drive 3, Singapore 117543, Singapore
[c] National University of Singapore (Suzhou) Research Institute, 377 Lin Quan Street, Suzhou Industrial Park, Suzhou, Jiangsu 215123, PR China
[d] Changzhou Qihui Management & Consulting Co., Ltd, Changzhou, Jiangsu 213000, PR China

ARTICLE INFO

Article history:
Received 22 August 2016
Received in revised form
5 January 2017
Accepted 23 January 2017
Available online 24 January 2017

Keywords:
Electrolysed water
Escherichia coli
Oxidative stress
NMR
Atomic force microscopy

ABSTRACT

Electrolysed water (EW) is an activated liquid with a high oxidation-reduction potential. EW causes oxidative damage to pathogenic microorganisms and as a result, may have utility in the food industry. The molecular mechanism of EW's action is not understood. In this study, we exposed *Escherichia coli* ATCC 25922 to a sub-lethal concentration of EW and examined structural and metabolic changes. Atomic force microscopy revealed that EW caused damage to *E. coli* membranes. To understand the metabolic responses to EW perturbations in of *E. coli*, multivariate data analysis of NMR spectroscopy demonstrated that EW significantly influenced the metabolic state. This included reducing nucleotide and amino acid biosynthesis, suppressing energy-associated metabolism, altering osmotic adjustment, and promoting fatty acid metabolism. The results enrich our understanding of *E. coli* metabolic changes caused by EW perturbation and support the effectiveness of the NMR metabolomics as a valuable tool to analyse and evaluate such a complex biological system.

1. Introduction

Electrolysed water (EW), also known as electrolysed oxidising water, has a strong bactericidal effect on many pathogenic bacteria (Gómez-López, Gil, Pupunat, & Allende, 2015; Huang, Hung, Hsu, Huang, & Hwang, 2008; Inatsu et al., 2010; Liu, Tan, Yang, & Wang, 2016). The sanitising action of acidic EW has been attributed to the high oxidation-reduction potential and the oxidative action of hypochlorous acid (Ding et al., 2015; Zhao, Zhang, & Yang, 2017). For this reason, EW is used as an alternative means to improve the shelf life and safety of food (Forghani et al., 2013).

Although the bactericidal effects of EW on microorganisms are well documented, there are few reports on the mechanism by which EW inactivates pathogens. Kim (Kim, Hung, & Brackett, 2000) suggested that the oxidation-reduction potential (ORP) of electrolysed water is a primary factor to consider in the inactivation of microorganisms. The high ORP of EW is possibly due to the oxygen released by the rupture of the unstable bond between chloric radicals and hydroxyl produced in electrolysis (Venkitanarayanan, Ezeike, Hung, & Doyle, 1999). This provides frequent changes in the electron flow in the cell to modify metabolic flux (Huang et al., 2008).

Microbial metabolomics has special biochemical significance in the study of cellular systems. Metabolomics is a useful and versatile tool for evaluating metabolic variations in microorganisms (Khoo et al., 2015). By monitoring the global metabolite profile, metabolomics provides a precise snapshot of the physicochemical state of the cell. In recent years, an increasing number of studies revealed the metabolic effects in response to exogenous stress factors (Jozefczuk et al., 2010; Metris, George, Mulholland, Carter, & Baranyi, 2014; Wu et al., 2013).

Microbial metabolomics analysis is a universally applicable approach capable of describing the cellular chemical fingerprint of bacteria. Changes in the metabolite composition of microorganisms in response to external stimuli can easily be measured using analytical methods coupled with multivariate statistical analysis

* Corresponding author. Food Science and Technology Programme, c/o Department of Chemistry, National University of Singapore, Singapore 117543, Singapore.
E-mail address: chmynghs@nus.edu.sg (H. Yang).

[1] Arushi is a high school student at United World College of South East Asia who conducts research attachment at NUS.

http://dx.doi.org/10.1016/j.lwt.2017.01.066
0023-6438/

(Park et al., 2016). Currently, two analytical technologies are routinely used to characterise the metabolomic profile in bacteria: nuclear magnetic resonance (NMR) and mass spectrometry (MS) (Coulier et al., 2006; Picone et al., 2013). NMR analysis can detect a wide range of low molecular weight metabolites in a single test and nowadays, NMR is the most frequently used method for the determination and quantitation of microbial metabolites.

Many studies have shown that EW can efficiently inactivate pathogens (Luo & Oh, 2016; Park, Guo, Rahman, Ahn, & Oh, 2009; Yang, Feirtag, & Diez-Gonzalez, 2013; Zhang & Yang, 2017). However, there are only a few reports on its mechanism of action. Specifically, comprehensive analyses of changes in bacterial metabolites under oxidative stress have not been performed. The primary aim of this study was to investigate the inactivation mechanism of EW in *E. coli*. We hypothesised that the global analysis of metabolites in *E. coli* would define a metabolic signature that would allow discrimination of oxidatively stressed cells from normal cells. To test this hypothesis, we used NMR to profile EW stressed *E. coli* and compared these to normal bacteria. Our results illustrate the potential for metabolic profiling to provide new biomarkers for microbiology studies.

2. Materials and Methods

2.1. Strains, media, and growth conditions

E. coli ATCC 25922 were inoculated from a glycerol stock and cultivated overnight at 37 °C in M9 minimal medium ($Na_2HPO_4 \bullet 2H_2O$, 7.1 g L^{-1}; KH_2PO_4, 3 g L^{-1}; NaCl, 0.5 g L^{-1}; NH_4Cl, 1 g L^{-1}), supplemented with 2 mL 1 M $MgSO_4$, 20 mL 20% (w/v) D-glucose, and 1 mL 0.1 M $CaCl_2$.

2.2. Count of surviving cells

The numbers of cells were determined before and after treatment. For bacterial viability experiments, *E. coli* ATCC 25922 cells were cultivated in M9 minimal media until an A_{600} of 0.4–0.5 was reached. Following this, the cells were washed twice with phosphate-buffered saline (PBS) buffer and re-suspended in the original volume of PBS buffer. The washed cells were distributed into tubes, after which EW (2, 4, 10, 20 mg/L free available chlorine (FAC)) was added and treated for 5 min. Cells were serially diluted in neutralizing buffer (BD Biosciences) and spread onto tryptic soy agar (TSA, Oxoid).

2.3. Morphology observation by atomic force microscopy (AFM)

E. coli suspension (10^8 CFU/mL) was first centrifuged at 10000 *g* for 1 min, then washed twice with PBS and re-dispersed in deionised (DI) water. EW was added into *E. coli* suspension at various concentrations and treated for 5 min. Untreated and treated *E. coli* were spread onto freshly cleaved mica sheets and air-dried in a laminar flow cabinet. Characterisation of *E. coli* morphology was carried out by TT- Atomic Force Microscope (AFM workshop, Signal Hill, CA, USA) that was equipped with a Sensaprobe TM190-A-15 tip (Applied Nanostructures, Mountain View, CA, USA), with settings of 512 pixels/line and 1 Hz scan rate. Gwyddion software was used to process the AFM images and to describe quantitatively the topography of the bacterial surface. Section analyses and root-mean-square roughness (RMS) were taken from the height images. RMS was calculated from two individual regions ($0.4 \times 0.4\ \mu m^2$), on the surface of one cell and roughness' results were average values taken from the central parts of at least 15 cells.

2.4. Extraction of intracellular metabolites

After 18–24 h, cells were diluted to 1:20 and cultivated at 37 °C in freshly prepared M9 minimal medium until an A_{600} of 0.5–0.6 was reached. A 200 mL of M9 aliquots containing *E. coli* were subject to two treatments: untreated control and exposure to EW stress (4 mg/L FAC) under short vortexing. *E. coli* was stressed at 37 °C for 30 min or 5 min was selected to evaluate the EW-related metabolic effects. The cell cultures were quenched by a brief incubation on ice, followed by centrifugation (12,000 *g*, 5 min, 4 °C). The supernatant was decanted. The cell pellet was subsequently washed three times with ice-cold PBS (pH 7.4) to remove the glucose and other components from the medium. This was to ensure that all detected metabolites were derived from the *E. coli* cell and not from the media. Cell pellets were again suspended in 600 μL extraction solution and sonicated on wet ice for 25 cycles with each cycle consisting of 5 s pulse and 10 s stops. The extraction solution was prepared by mixing equal volume of NaH_2PO_4-K_2HPO_4 buffer (0.1 mol/L, pH 7.4, containing 10% D_2O) and acetonitrile. The metabolites from lysed cells were obtained by centrifugation at 1000*g* at 4 °C for 10 min. The remaining solid residues were further extracted using the same extract solution and homogenized using a vortex. The secondary supernatant was collected after centrifugation and pooled with the first one. The pooled supernatant was condensed by vacuum to remove acetonitrile. The samples were stored at −80 °C for NMR analysis.

2.5. NMR acquisition

For NMR analysis, 550 μL of the extract was transferred into a 5 mm NMR tube. All NMR measurements were performed at 298 K using a Bruker DRX-500 NMR Spectrometer equipped with a Triple Inverse Gradient (TXI) probe (Bruker, Germany). For all samples, the ^1H NMR spectra were acquired using a first increment of NOESY pulse sequence (recycle delay-90°-t_1-90°-t_m-90°-acquisition). Water suppression was achieved with a weak continuous wave irradiation during both, the recycle delay (RD, 2 s) and the mixing time (t_m, 100 ms). The t_1 was set to 6.5 μs and the 90° pulse length was adjusted to approximately 10 μs. Sixty-four transients were collected into 32 k data points for each spectrum with a spectral width of 17 ppm and an acquisition time of 1.36 s. An exponential window function with a line broadening factor of 1 Hz was applied to all free induction decays (FIDs) prior to Fourier transformation (FT).

2.6. Spectral processing and statistical analysis

AFM results were statistically analysed by Analysis of Variance using SPSS statistical software (IBM, Armonk, NY, USA). A two-tailed Student's t-test was used to determine the statistical significance where $P < 0.05$ was considered to be statistically significant.

The resulting NMR spectra were manually phased and baseline corrected using TopSpin 4.2 (Bruker Biospin, Rheinstetten, Germany) and data reduction was accomplished by dividing the spectrum from δ 8.5 to 0.5 into regions bucket with width of 0.02 ppm using Mnova (Mestreab Research SL, Santiago de Compostela, Spain). The solvents signals (water and acetonitrile) were excluded and the standardized binned data was used for multivariate data analysis. The spectral dataset was then constructed and imported into a SIMCA-P^+ software (version 13.0, Umetrics, Sweden) for multivariate analysis. Firstly, the principal component analysis (PCA) of the ^1H NMR spectra was performed to visualise the general structure of each data set and to identify any abnormalities within the data set. Data sets were then subject to orthogonal partial least squares discriminant analysis (OPLS-DA),

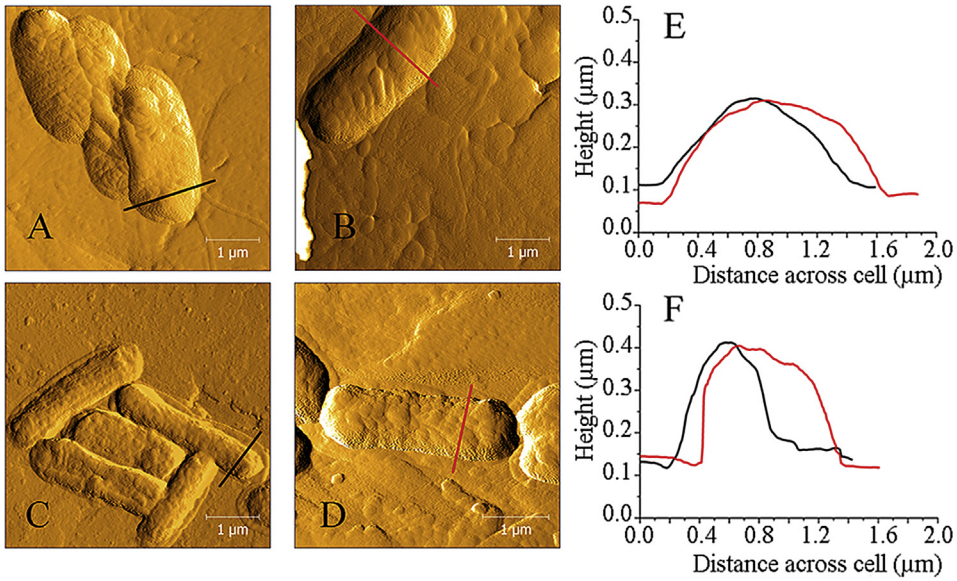

G

E.coli	Width (μm)	Height (μm)	W/H ratio	RMS roughness (nm)[a]
Control	1.51 ± 0.10	0.23 ± 0.03	6.53 ± 0.34	10.96 ±1.48
EW	0.92 ± 0.02*	0.30 ± 0.04 *	3.16 ± 0.47 *	23.52 ± 4.38 *

Values are mean ± SD and statistically analysed by Student's t-test.
* $P < 0.05$ compared with the control group.
[a] $0.4 \times 0.4\ \mu m^2$ area was used to measure the cell surface RMS roughness

Fig. 1. AFM Morphology of fresh and treated *E. coli* by EW: untreated (a–b), EW treated (c–d). The profiles of the black and red lines were shown in the figures: untreated (e), EW treated (f). The cell morphology summary of *E.coli* was shown in figure (g) at the bottom. (For interpretation of the references to colour in this figure legend, the reader is referred to the web version of this article.)

an extension of the supervised partial least squares regression (PLS regression) method in order to increase the quality of the classification model (Sinanoglou et al., 2014). OPLS-DA facilitates model interpretation by separating the systematic variation in X into two parts, one that is linearly related to Y and one that is orthogonal to Y (Piccinonna et al., 2016). Loading and coefficient plots were extracted to reveal the variables that bear class discriminating power. S-line plots were extracted in order to detect the metabolites that influence the group membership (colour coding visualisation). Moreover, variable importance in projection (VIP) was performed on the preprocessed spectra using the algorithms included in the OPLS-toolbox. This was to reveal the metabolites primarily affecting the samples' differentiation. Specifically, terms with a VIP value higher than 1 influenced mostly the extracted OPLS models (Fotakis & Zervou, 2016).

3. Results and discussion

3.1. E. coli viability

E. coli was cultured up to an A_{600} of 0.4–0.5 and EW was then added at concentrations of 2, 4, 10 and 20 mg/L. *E. coli* were exposed to EW for 5 min at 37 °C. No significant difference in viable cell number was noted between the control samples (8.25 ± 0.46 log CFU/mL) and those treated with 2 mg/L EW. However, the viable cell number was slightly reduced (7.47 ± 0.02 log CFU/mL) by the addition of 4 mg/L EW, while 10 mg/L EW decreased it further to 4.73 ± 0.27 log CFU/mL. EW at the maximum concentration tested (20 mg/L) decreased the viable cell number to below the detection limit (1 log CFU/mL). Therefore, the first indication of cell stress occurred at 4 mg/l EW while the cells still showed high viability.

3.2. Morphology results from Atomic Force Microscopy (AFM)

AFM has provided a way to investigate the nanoscale surface characterisation of bacteria with high resolution (Yang, 2014;

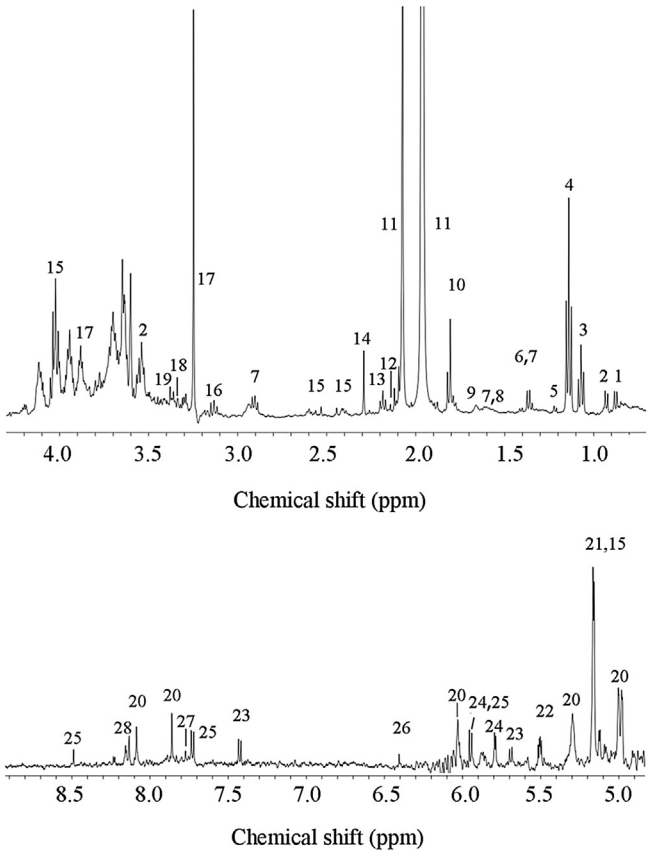

Fig. 2. Two typical ^{1}H NMR spectra of *E. coli* extracts from the untreated control group. Metabolites: 1. isoluecine, 2. leucine, 3. valine, 4. β-hydroxybutyrate, 5. N-acetyl alanine, 6. alanine, 7. lysine, 8. arginine 9. putrescine, 10. acetate, 11. glutamate, 12. γ-aminobutyrate, 13. β-aminoadipate, 14. succinate, 15. glyceric acid, 16. phosphorylcholine, 17. betaine, 18. methanol, 19. glycine, 20. adenosine 2′-3′-cyclic phosphate, 21. α-glucose, 22. ribose-5-phosphate, 23. uridine, 24. cytidine, 25. nicotinate, 26. fumarate, 27. xanthine, 28. hypoxanthine.

Zhang & Yang, 2017). AFM has the capability to investigate microorganisms at level as even single microbe. AFM was used to reveal morphological changes in *E. coli* following treatment with EW. Fig. 1 shows the morphology of untreated *E. coli* compared to cells treated with EW for 5 min. In the control group, the cell membrane appeared intact and there were no obvious indentations or grooves on the surface. The bacterial flagella could be clearly observed. After treatment with EW, flagella were no longer visible and the *E. coli* showed a compromised membrane. A small amount of intracellular material could, in fact, be observed effusing from the cell. Despite this, the cell membrane was not found collapsed, indicating that most of the intracellular components remained inside the bacterial cell.

The *E. coli* AFM images were analysed to obtain height and width measurements and were then used to quantitate the morphological changes. The width/height (W/H) ratio was used as an index to indicate preservation of bacterial cell shape following EW treatment, since for rod-shaped bacteria, a W/H ratio close to one is representative of a healthy cell (Chao & Zhang, 2011). The results show that the *E. coli* W/H ratio was reduced by more than half following EW treatment compared to untreated cells. Treatment with EW also induced elevated structures within the cell since the width decreased by 35.33% while the height increased by 40.90%.

Surface roughness, in terms of the RMS value, is another quantitative index used to assess bacterial surface morphology, indicating the standard deviation of all height values within the given area (Camesano, Natan, & Logan, 2000). As shown in Fig. 1, untreated *E. coli* cells had relatively smooth surfaces (RMS = 10 ± 1.5 nm) with small spherical structures typical of the morphology found on the surface of Gram-negative bacteria. These spherical structures have been observed in previous studies and are thought to be lipopolysaccharides (LPS) (Tang, McEwen, Wu, Miller, & Zhou, 2013) as well as protein aggregates embedded in the exposed lipopolysaccharide layer (Micic et al., 2004); they form the first line of defence for Gram-negative bacteria. When treated with EW at 4 mg/L, wrinkled bundles and lesions were observed and an increased RMS of 23 ± 4.4 nm was noticed. This rough surface and deformed cellular structure demonstrate that EW stress causes morphological changes in *E. coli*.

3.3. NMR profile

The typical ^{1}H NMR spectra of *E. coli* extracts prepared from untreated control cells are shown in Fig. 2. Several NMR databases containing the ^{1}H spectra of biological compounds have recently been made accessible, significantly helping the assignment process. The *E. coli* Metabolome Database (ECMDB, http://www.ecmdb.ca) is a comprehensively annotated metabolomics database containing detailed information about the metabolome of *E. coli* (Guo et al., 2013). Twenty-eight key metabolites were identified from the NMR spectra and the most predominant ones included a wide range of amino acids, nucleotides, organic acids, and others. Although peak overlap is one of the major factors that can complicate the analysis of biomolecules, the resolution of overlapping signals in NMR spectrum is not always such a critical issue as it is in mass spectrometry (MS) chromatographic methods (Puig-Castellví, Alfonso, Piña, & Tauler, 2015). Since each metabolite always contains more than one identical resonance signal, if an overlapping region cannot be resolved, it is possible that the resonance signals comprised in that region come from metabolites with equivalent signals in other regions of the spectrum, making the related metabolites identifiable. In addition, NMR has the inherent advantage of providing simultaneous access to both qualitative and absolute quantitative information, whereas MS requires a calibration curve for each compound, due to the variable ionisation rates of different metabolites.

The spectrum of each extract shows, in the range between 0 and 4 ppm, a preponderance of signals related to organic acids and amino acids. In the region between 5 and 8.5 ppm, as expected from the use of acetonitrile for extraction, aromatic compounds such as adenosine 2′-3′-cyclic phosphate (2′, 3'-cAMP), as well as uridine and cytidine nucleotides were noted. These metabolites were readily assignable on the basis of database or literature data. The key diagnostic metabolites are summarised in Table 1.

3.4. Chemometrics: metabolic alteration

The overall cellular processes affected by EW stress were captured by the whole metabolome analysis. Initially, PCA analysis was performed to generate an overview of the metabolic alterations during 30 min stress. The metabolic trajectories of untreated control and stressed groups were drawn by taking the mean position in the scores plot for samples and connecting the coordinates chronologically (Fig. 3). As shown in Fig. 3, the score trajectory indicated relative stable metabolic profiles of the control *E. coli* during the first 5 min and the deviation from the stable space can be observed at 30 min. The trajectories of untreated control and EW-stressed were similar in the change pattern along the first principle component (PC1), which indicated the comparable metabolic profiles for the control and stressed groups. However, it

Table 1
^{1}H NMR chemical shifts of low-molecular-weight metabolites.

No.	Metabolic compounds	Chemical shifts (ppm) and multiplicity
1	Isoleucine	0.89 (t)
2	Leucine	0.93 (d), 3.53 (d)
3	Valine	1.06 (d)
4	β-hydroxybutyrate	1.12 (d)
5	N-acetyl alanine	1.21 (s)
6	Alanine	1.38 (d)
7	Lysine	1.35 (t), 1.63 (t), 2.91 (t)
8	Arginine	1.58 (d)
9	Putrescine	1.65 (t)
10	Acetate	1.80 (s)
11	Glutamate	1.95 (d), 2.08 (d)
12	γ-aminobutyrate	2.17 (t)
13	β-aminoadipate	2.18 (t)
14	Succinate	2.29 (s)
15	Glyceric acid	4.13 (m)
16	Phosphorylcholine	3.13
17	Betaine	3.25 (s), 3.89 (s)
18	Methanol	3.33 (s)
19	Glycine	3.39 (s)
20	Adenosine 2′-3′-cyclic phosphate	5.00 (m), 5.30 (m), 6.03 (m), 7.85 (m), 8.09 (m)
21	α-glucose	5.17 (d)
22	Ribose-5-phosphate	5.50 (m)
23	Uridine	5.69 (d) 5.79 (d), 7.42 (d)
24	Cytidine	5.79 (d), 5.95 (d)
25	Nicotinate	5.95 (d), 7.72 (d), 8.49 (d)
26	Fumarate	6.40 (s)
27	Xanthine	7.78 (s)
28	Hypoxanthine	8.12 (s)

Multiplicity: s-singlet, d-doublet, t-triplet, q-quartet, m-multiplet.

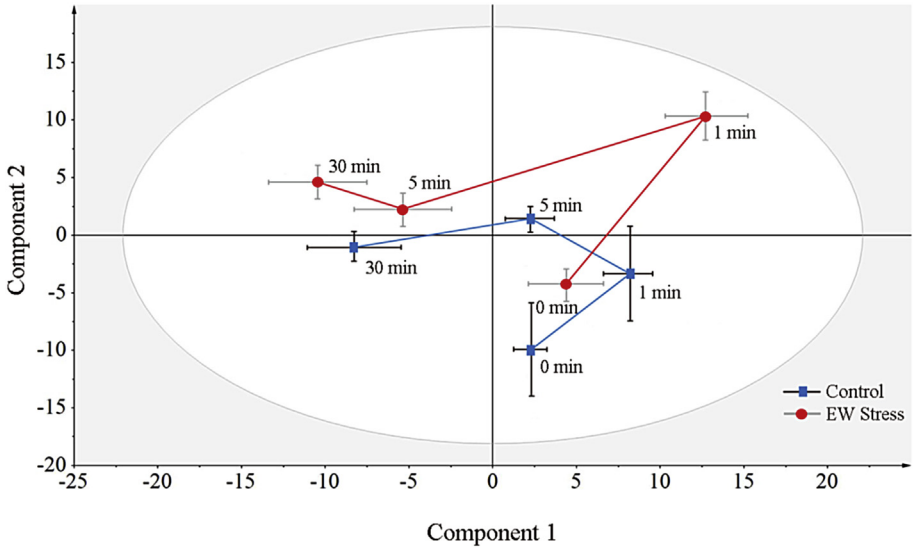

Fig. 3. Trajectory plot derived from PCA of ^{1}H NMR spectra of *E.coli* extracts. (square: control group; circle: EW stressed group).

is worth noting that the points of mean score of the stressed group moved further away from the initial state with respect to the score at 0 min. The EW-related metabolic effects were further evaluated by OPLS-DA. This was accomplished using the score and correlation coefficient plots of selected sampling time point (5 min) for which are shown in Fig. 4. OPLS-DA was capable of discriminating between untreated and EW stressed *E. coli*. This observation showed that NMR is a powerful tool that can be used to define EW stress. Furthermore, the s-line (Fig. 4B) identifies the chemical shifts based on correlation coefficient values responsible for the differentiation using a colour code that indicates the weights of the discriminatory variables. Specifically, as the colour of the peak gradually changes from blue to red, the absolute value of the correlation coefficient increases from 0 to 1, indicating the resonances important for discriminating the metabolite profiles of pairwise untreated and EW stressed group.

According to the S-line plot, chemical bins of 0.8–3 ppm represented the most altered metabolites, and these can mostly be assigned to amino acids. Among biological molecules, amino groups, peptide bonds (amide bond), and thiol groups are susceptible to oxidation by free radicals (Nightingale et al., 2000). Amino acids have been previously reported to be useful as potential markers of oxidative stress because they contain reactive residues. Free amino groups (e.g. lysine) can be converted into unstable

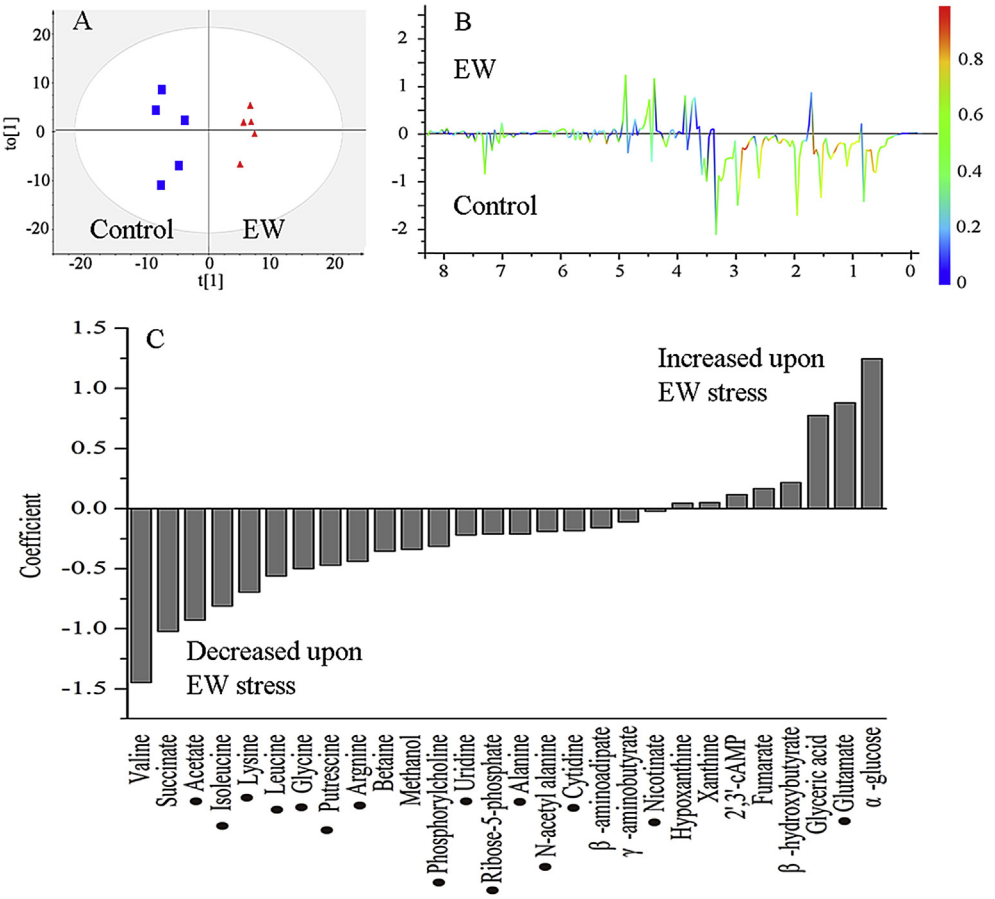

Fig. 4. The OPLS score (A), S-line (B) and coefficient (C) plots comparing the metabolic profile of EW treated and control *E. coli*. The black dots indicate which metabolites contribute significantly to the OPLS-DA models (VIP > 1, see Materials and Methods for further details). R^2 X = 0.797, Q^2 Y = 0.687.

chloramines by reaction with $HOCl/OCl^-$ and further broken down to nitrogen-centred radicals via haemolysis of N-Cl bonds, which are the key species involved in the fragmentation of proteins (Hawkins, Pattison, & Davies, 2002).

The coefficient plot (Fig. 4C) shows the increase or decrease in concentration for each of the metabolites identified. The analysis shows that untreated and EW stressed *E. coli* are different at the biochemical level. The levels of amino acids including isoleucine, lysine, leucine, arginine and alanine were significantly lower in EW treated cells. The levels of other metabolites including succinate, acetate, putrescine and glutamate were also severely reduced, highlighting the general changes in the metabolic network caused by EW.

In order to identify the metabolites that were most significant for allowing for discrimination of EW-elicited effects, VIP scores were calculated as a composite measure of a metabolite's importance in explaining the statistical variance and the predictive value of the model. In the OPLS-DA analysis, the VIP scores allow a ranking of the metabolites ordered according to how much they influenced the separation of the two treatment groups. Variables with a VIP score greater than 1 are the most relevant for explaining Y and can be considered important in a given model (Kuligowski, Quintás, Herwig, & Lendl, 2012). The metabolites with VIP scores greater than 1 are depicted with black dots in Fig. 4C. The results show that changes in the levels of acetate, isoleucine, lysine, leucine, glycine, putrescine, arginine, phosphorycholine, uridine, ribose-5-phosphate, alanine, N-acetyl alanine, cytidine, nicotinate and glutamate upon addition of EW were important in discriminating EW treated *E. coli* from untreated *E. coli* in the OPLS-DA model. Accordingly, the most relevant metabolites were phosphorylcholine and ribose-5-phosphate. Phosphorylcholine is a key membrane phospholipid precursor and ribose-5-phosphate is a key intermediate in carbohydrate and nucleotide metabolism.

3.5. Pathway analysis

To identify the relevant metabolic pathways involved in the metabolic response to EW stress, a differential metabolite pathway analysis was performed using MetaboAnalyst 3.0 (Fig. 5). As a result, thirty-two pathways were predicted and five pathways were suggested to be associated with the response to EW ($P < 0.05$). These pathways included aminoacyl-tRNA biosynthesis, valine, leucine and isoleucine biosynthesis and degradation, glycine, serine and threonine metabolism, alanine, aspartate and glutamate metabolism, butanoate metabolism, and arginine and proline metabolism. A complete list of pathway analysis results can be found in Table 2.

Oxidative stress occurs when an imbalance arises between the production and removal of the reactive oxygen species in the bacterial environment. Fig. 6 reveals an overall profile of the metabolic perturbations caused by EW stress in *E. coli*. The results demonstrate that *E. coli* appears to react to oxidative stress by altering general metabolic pathways, including nucleotide and amino acid metabolism, fatty acid metabolism, energy metabolism and carbohydrate metabolism.

Consistent with the decrease in the levels of metabolites related

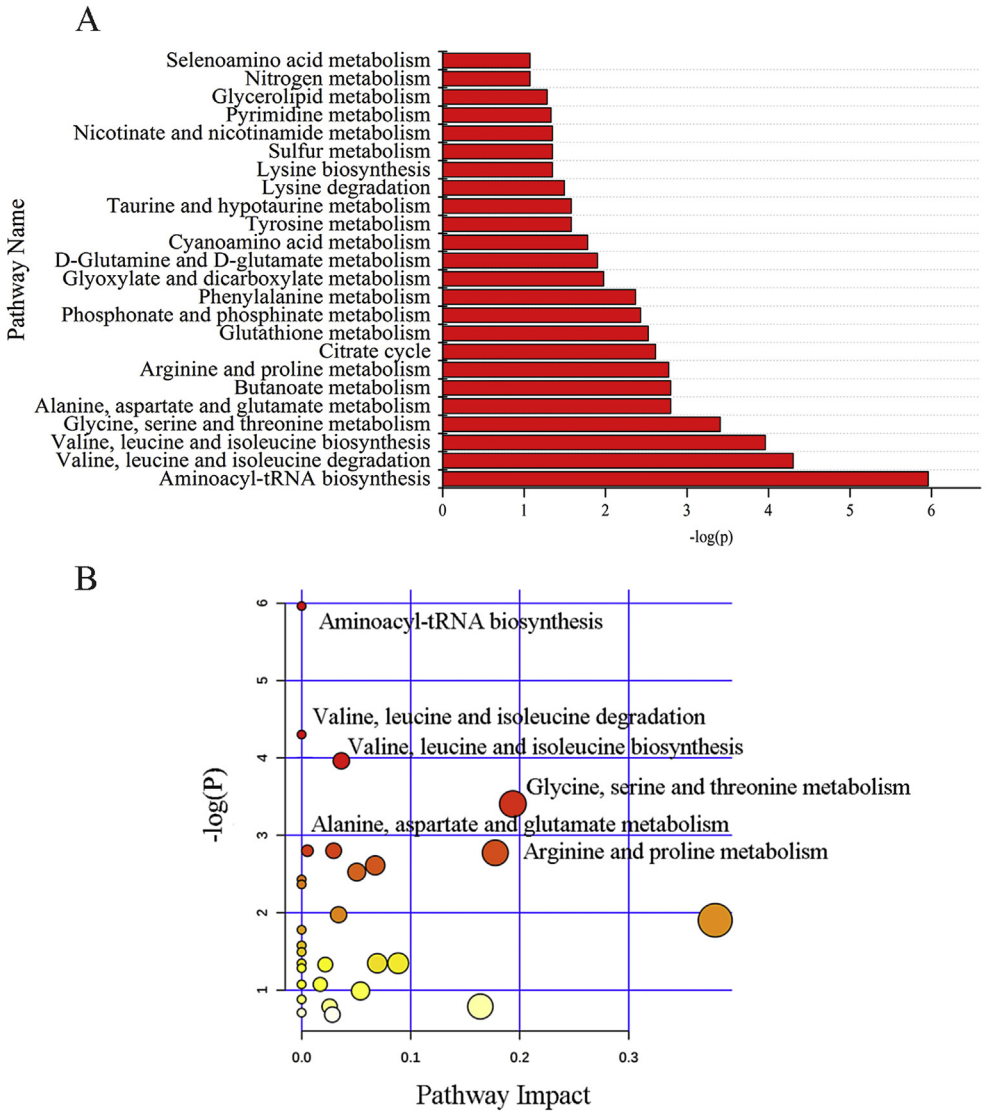

Fig. 5. Pathways analysis by using the MetaboAnalyst. (A) Summary plot for metabolite set enrichment analysis of metabolic response to EW stress. (B) Overview of pathway analysis offers a metabolomics view, which displays all matched pathways as circles. The colour and size of each circle is based on the p value and the pathways impact value, respectively.

to glycolysis, the pentose phosphate pathway was found to be one of the pathways most affected by EW-induced oxidative stress. Particularly noteworthy is the decrease in levels of ribose-5-phosphate, which is a key precursor in biosynthesis of nucleotides. The decrease in nucleotide biosynthesis is also often strongly reflected at the transcript level, being one of the most pronounced responses common to diverse stress conditions (Gasch et al., 2000). Therefore, it was not surprising that the levels of cytidine and uridine also decreased since these were predicted to decrease DNA and RNA biosynthesis.

EW stress also decreased the levels of betaine (data not shown), which is believed to be the most active naturally occurring osmoprotectant molecule in *E. coli* (Ly, Henderson, Lu, Culham, & Wood, 2004). The decrease in amino acid levels following EW oxidative stress is in agreement with amino acid synthesis being very sensitive to oxidation (Jozefczuk et al., 2010). In addition, wide-ranging oxidative stress, such as that caused by EW, may induce the amino acid oxidase system instead of the more common glucose oxidase system (Lushchak, 2011).

The depleted levels of amino acids also indicate that EW causes osmotic stress. Numerous studies have suggested that a number of amino acid function to maintain the normal osmolality of the cytoplasm, retain cellular water and prevent the collapse of subcellular structures (Ye et al., 2012).

In response to oxidative stress, bacteria may react rapidly to attempt to repair the damage incurred, using, for example, inducible genetic systems such as the oxyR regulon. Bearson demonstrated that the glutamate decarboxylase system could provide *E. coli* with protection against oxidative stress during acid challenge (Bearson, Lee, & Casey, 2009). In addition, γ-aminobutyric acid (GABA) is a four carbon, non-protein, amino acid that can play a role in antioxidant defence. The synthesis of GABA is catalysed by glutamate decarboxylase. In this study, a marked elevation of glutamate was observed in EW treated *E. coli* along with a concomitant decrease in succinate derived from α-ketoglutarate. Based on these findings, it is likely that the increased levels of glutamate are used for synthesis of GABA during EW stress.

Under adverse environmental conditions, microbes adopt an energy saving strategy to maintain sufficient energy for growth and survival. Many microbes have evolved to regulate the metabolic

Table 2
List of metabolic pathway by enrichment analysis for the metabolites.

Pathway name	Total	Hits	Raw *P*	FDR
Aminoacyl-tRNA biosynthesis	66	6	0.00258	0.224
Valine, leucine and isoleucine degradation	23	3	0.0135	0.418
Valine, leucine and isoleucine biosynthesis	26	3	0.0190	0.418
Glycine, serine and threonine metabolism	32	3	0.0332	0.481
Alanine, aspartate and glutamate metabolism	18	2	0.0407	0.603
Butanoate metabolism	18	2	0.0411	0.603
Arginine and proline metabolism	41	3	0.0623	0.603
Citrate cycle (TCA cycle)	20	2	0.0734	0.628
Glutathione metabolism	21	2	0.0800	0.628
Phosphonate and phosphinate metabolism	4	1	0.0881	0.628
Phenylalanine metabolism	23	2	0.0938	0.628
Glyoxylate and dicarboxylate metabolism	29	2	0.139	0.862
D-Glutamine and D-glutamate metabolism	7	1	0.149	0.865
Cyanoamino acid metabolism	8	1	0.169	0.917
Tyrosine metabolism	10	1	0.206	0.997
Taurine and hypotaurine metabolism	10	1	0.206	0.997
Lysine degradation	11	1	0.224	0.998
Lysine biosynthesis	13	1	0.260	0.998
Sulphur metabolism	13	1	0.260	0.998
Nicotinate and nicotinamide metabolism	13	1	0.260	0.998
Pyrimidine metabolism	44	2	0.264	0.998
Glycerolipid metabolism	14	1	0.277	1
Nitrogen metabolism	18	1	0.341	1
Selenoamino acid metabolism	18	1	0.341	1
Propanoate metabolism	20	1	0.372	1
Pantothenate and CoA biosynthesis	23	1	0.414	1
Pyruvate metabolism	26	1	0.454	1
Pentose phosphate pathway	26	1	0.454	1
Glycolysis or Gluconeogenesis	29	1	0.492	1
Purine metabolism	73	2	0.504	1

FDR: False Discovery Rate, Raw *P*: Raw *P* value.

expenditure of the cell and thereby reduce the energy burden of metabolism. Our results showed a significant drop in glucose levels in EW stressed cells. It is well known that glucose is the preferred carbon and energy source for *E. coli*, therefore it is likely that EW restricted this energy resource. Besides the decreased consumption of glucose, the lower level of acetate indicated the inhibition of phosphate acetyltransferase-acetate kinase, an important enzyme in the carbon fixation pathway. Taken together, these observed metabolic changes, namely the decrease in the pentose phosphate pathway and glycolytic pathways, are in general agreement with the energy conservation strategy previously reported for the transcriptomic response (Jozefczuk et al., 2010).

Fatty acids are also major targets during oxidative stress. Free radicals can directly fatty acid resulting in lipid peroxidation (Cabiscol, Tamarit, & Ros, 2000). In this study, the higher level of 3-hydroxybutyrate, one of the three key ketone bodies, was observed, indicating the transient increase in fatty acid metabolism as a response to EW treatment. This can be illustrated by the sigma factor Repos, which is upregulated by elevated concentrations of the global regulator (p)ppGpp ((guanosine 5-triphosphate, 3-diphosphate) guanosine 3, 5-bispyrophosphate) (Janßen& Steinbüchel, 2014). Repos, which can regulate ~200 genes, is involved in multiple stress responses, including responses to acid, heat, oxidative stress, UV light, or starvation (Chiang & Schellhorn, 2012; Small, Blankenhorn, Welty, Zinser, & Slonczewski, 1994).

Here, we have found a panel of metabolites, which we consider to have a strong association with EW stress. These metabolites show either an increase or a decrease in EW treated *E. coli*. However, further investigation of the metabolic response induced by oxidative stress is needed in order to elucidate the bactericidal mechanism of EW, especially for processing organic produce (Yu & Yang, 2017).

4. Conclusions

The present work shows that information on cellular metabolites obtained by NMR analysis might serve as a basis for future mechanistic studies. In this context, we have demonstrated changes in amino acids, organic acids and nucleotides in *E. coli* after EW stress. Analysis of the data using OPLS-DA was particularly useful. The target of such analysis is to build linear combinations of the original data, but orthogonal to each other. This study is an example of how metabolomics, the study of multiple metabolic changes caused by a biological perturbation, may easily enrich the knowledge in a field of increasing importance such as the use of EW in food processing. It should be noted that the interpretation of metabolomics data is not always straightforward because of its

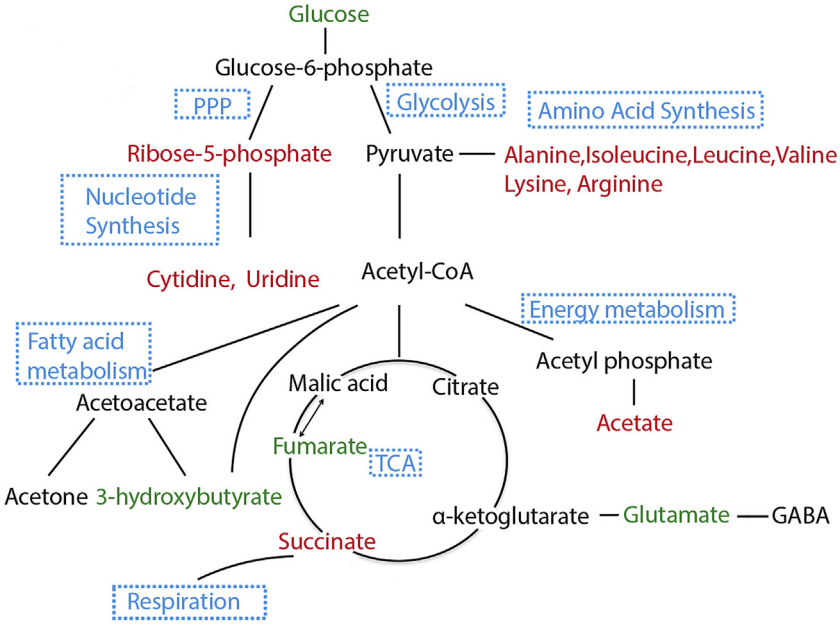

Fig. 6. Metabolic pathways affected by EW stress. Metabolites coloured in green and red represent a higher and lower level in EW stressed *E. coli* extracts respectively compared to control *E. coli*. Metabolites in black were not detected. (For interpretation of the references to colour in this figure legend, the reader is referred to the web version of this article.)

inherent complexity. We believe that the uses of novel omics approaches (as depicted by advanced NMR or mass spectrometry methods), greatly aid in the assessment of low-molecule-weight metabolite targets and biomarker discovery. For further validation, these potential biomarkers could be readily determined by specific chemical quantification approaches such as targeted chromatography.

Acknowledgements

We acknowledge the financial support by Singapore Ministry of Education Academic Research Fund Tier 1 (R-143-000-583-112), Projects 31371851 and 31071617 supported by NSFC, Natural Science Foundation of Jiangsu Province (BK20141220), and an industry project (R-143-000-616-597) contributed by Changzhou Qihui Management & Consulting Co., Ltd.

References

Bearson, B. L., Lee, I. S., & Casey, T. A. (2009). *Escherichia coli* O157:H7 glutamate- and arginine-dependent acid-resistance systems protect against oxidative stress during extreme acid challenge. *Microbiology, 155*, 805–812.

Cabiscol, E., Tamarit, J., & Ros, J. (2000). Oxidative stress in bacteria and protein damage by reactive oxygen species. *International Microbiology, 3*, 3–8.

Camesano, T. A., Natan, M. J., & Logan, B. E. (2000). Observation of changes in bacterial cell morphology using tapping mode atomic force microscopy. *Langmuir, 16*, 4563–4572.

Chao, Y., & Zhang, T. (2011). Optimization of fixation methods for observation of bacterial cell morphology and surface ultrastructures by atomic force microscopy. *Applied Microbiology and Biotechnology, 92*, 381–392.

Chiang, S. M., & Schellhorn, H. E. (2012). Regulators of oxidative stress response genes in *Escherichia coli* and their functional conservation in bacteria. *Archives of Biochemistry and Biophysics, 525*, 161–169.

Coulier, L., Bas, R., Jespersen, S., Verheij, E., van der Werf, M. J., & Hankemeier, T. (2006). Simultaneous quantitative analysis of metabolites using ion-pair liquid chromatography-electrospray ionization mass spectrometry. *Analytical Chemistry, 78*, 6573–6582.

Ding, T., Ge, Z., Shi, J., Xu, Y. T., Jones, C. L., & Liu, D. H. (2015). Impact of slightly acidic electrolyzed water (SAEW) and ultrasound on microbial loads and quality of fresh fruits. *LWT - Food Science and Technology, 60*, 1195–1199.

Forghani, F., Rahman, S. M. E., Park, M. S., Park, J. H., Park, J., Song, K. B., et al. (2013). Ultrasonication enhanced low concentration electrolyzed water efficacy on bacteria inactivation and shelf life extension on lettuce. *Food Science and Biotechnology, 22*, 131–136.

Fotakis, C., & Zervou, M. (2016). NMR metabolic fingerprinting and chemometrics driven authentication of Greek grape marc spirits. *Food Chemistry, 196*, 760–768.

Gasch, A. P., Spellman, P. T., Kao, C. M., Carmel-Harel, O., Eisen, M. B., Storz, G., et al. (2000). Genomic expression programs in the response of yeast cells to environmental changes. *Molecular Biology of the Cell, 11*, 4241–4257.

Gómez-López, V. M., Gil, M. I., Pupunat, L., & Allende, A. (2015). Cross-contamination of *Escherichia coli* O157:H7 is inhibited by electrolyzed water combined with salt under dynamic conditions of increasing organic matter. *Food Microbiology, 46*, 471–478.

Guo, A. C., Jewison, T., Wilson, M., Liu, Y., Knox, C., Djoumbou, Y., et al. (2013). ECMDB: The *E. coli* metabolome database. *Nucleic Acids Research, 41*, D625–D630.

Hawkins, C. L., Pattison, D. I., & Davies, M. J. (2002). Reaction of protein chloramines with DNA and nucleosides: Evidence for the formation of radicals, protein-DNA cross-links and DNA fragmentation. *The Biochemical Journal, 365*, 605–615.

Huang, Y. R., Hung, Y. C., Hsu, S. Y., Huang, Y. W., & Hwang, D. F. (2008). Application of electrolyzed water in the food industry. *Food Control, 19*, 329–345.

Inatsu, Y., Kitagawa, T., Bari, M. L., Nei, D., Juneja, V., & Kawamoto, S. (2010). Effectiveness of acidified sodium chlorite and other sanitizers to control *Escherichia coli* O157:H7 on tomato surfaces. *Foodborne Pathogens and Disease, 7*, 629–635.

Janßen, H. J., & Steinbüchel, A. (2014). Fatty acid synthesis in *Escherichia coli* and its applications towards the production of fatty acid based biofuels. *Biotechnology for Biofuels, 7*(1), 1.

Jozefczuk, S., Klie, S., Catchpole, G., Szymanski, J., Cuadros-Inostroza, A., Steinhauser, D., et al. (2010). Metabolomic and transcriptomic stress response of *Escherichia coli*. *Molecular Systems Biology, 6*, 364.

Khoo, L. W., Mediani, A., Zolkeflee, N. K. Z., Leong, S. W., Ismail, I. S., Khatib, A., et al. (2015). Phytochemical diversity of *Clinacanthus nutans* extracts and their bioactivity correlations elucidated by NMR based metabolomics. *Phytochemistry Letters, 14*, 123–133.

Kim, C., Hung, Y. C., & Brackett, R. E. (2000). Efficacy of electrolyzed oxidizing (EO) and chemically modified water on different types of foodborne pathogens. *International Journal of Food Microbiology, 61*(2), 199–207.

Kuligowski, J., Quintás, G., Herwig, C., & Lendl, B. (2012). A rapid method for the differentiation of yeast cells grown under carbon and nitrogen-limited conditions by means of partial least squares discriminant analysis employing infrared micro-spectroscopic data of entire yeast cells. *Talanta, 99*, 566–573.

Liu, Q., Tan, C., Yang, H., & Wang, S. (2016). Treatment with low-concentration acidic electrolysed water combined with mild heat to sanitise fresh organic broccoli (*Brassica oleracea*). *LWT-Food Science and Technology*. http://dx.doi.org/10.1016/j.lwt.2016.11.012.

Luo, K., & Oh, D. H. (2016). Inactivation kinetics of *Listeria monocytogenes* and *Salmonella enterica* serovar *Typhimurium* on fresh-cut bell pepper treated with slightly acidic electrolyzed water combined with ultrasound and mild heat. *Food Microbiology, 53*, 165–171.

Lushchak, V. I. (2011). Adaptive response to oxidative stress: Bacteria, fungi, plants and animals. Comparative Biochemistry and Physiology Part C. *Toxicology & Pharmacology, 153*, 175–190.

Ly, A., Henderson, J., Lu, A., Culham, D. E., & Wood, J. M. (2004). Osmoregulatory systems of *Escherichia coli*: Identification of betaine-carnitine-choline transporter family member betU and distributions of betU and trkG among pathogenic and nonpathogenic isolates. *Journal of Bacteriology, 186*, 296–306.

Metris, A., George, S. M., Mulholland, F., Carter, A. T., & Baranyi, J. (2014). Metabolic shift of *Escherichia coli* under salt stress in the presence of glycine betaine. *Applied and Environmental Microbiology, 80*, 4745–4756.

Micic, M., Hu, D., Suh, Y. D., Newton, G., Romine, M., & Lu, H. P. (2004). Correlated atomic force microscopy and fluorescence lifetime imaging of live bacterial cells. *Colloids and Surfaces B: Biointerfaces, 34*, 205–212.

Nightingale, Z. D., Lancha, A. H., Jr., Handelman, S. K., Dolnikowski, G. G., Busse, S. C., Dratz, E. A., et al. (2000). Relative reactivity of lysine and other peptide-bound amino acids to oxidation by hypochlorite. *Free Radical Biology and Medicine, 29*, 425–433.

Park, Y. B., Guo, J. Y., Rahman, S. M. E., Ahn, J., & Oh, D. H. (2009). Synergistic effect of electrolyzed water and citric acid against *Bacillus Cereus* cells and spores on cereal grains. *Journal of Food Science, 74*, 185–189.

Park, S. E., Yoo, S. A., Seo, S. H., Lee, K. I., Na, C. S., & Son, H. S. (2016). GC-MS based metabolomics approach of Kimchi for the understanding of *Lactobacillus plantarum* fermentation characteristics. *LWT - Food Science and Technology, 68*, 313–321.

Piccinonna, S., Ragone, R., Stocchero, M., Coco, L. D., Pascali, S. A., Schena, F. P., et al. (2016). Robustness of NMR-based metabolomics to generate comparable data sets for olive oil cultivar classification. An inter-laboratory study on Apulian olive oils. *Food Chemistry, 199*, 675–683.

Picone, G., Laghi, L., Gardini, F., Lanciotti, R., Siroli, L., & Capozzi, F. (2013). Evaluation of the effect of carvacrol on the *Escherichia coli* 555 metabolome by using ^{1}H-NMR spectroscopy. *Food Chemistry, 141*, 4367–4374.

Puig-Castellví, F., Alfonso, I., Piña, B., & Tauler, R. (2015). A quantitative ^{1}H NMR approach for evaluating the metabolic response of *Saccharomyces cerevisiae* to mild heat stress. *Metabolomics, 11*, 1612–1625.

Sinanoglou, V. J., Kokkotou, K., Fotakis, C., Strati, I., Proestos, C., & Zoumpoulakis, P. (2014). Monitoring the quality of γ-irradiated macadamia nuts based on lipid profile analysis and Chemometrics. Traceability models of irradiated samples. *Food Research International, 60*, 38–47.

Small, P., Blankenhorn, D., Welty, D., Zinser, E., & Slonczewski, J. L. (1994). Acid and base resistance in *Escherichia coli* and *Shigella flexneri*: Role of rpoS and growth pH. *Journal of Bacteriology, 176*, 1729–1737.

Tang, M., McEwen, G. D., Wu, Y., Miller, C. D., & Zhou, A. (2013). Characterization and analysis of mycobacteria and Gram-negative bacteria and co-culture mixtures by Raman microspectroscopy, FTIR, and atomic force microscopy. *Analytical and Bioanalytical Chemistry, 405*, 1577–1591.

Venkitanarayanan, K. S., Ezeike, G. O., Hung, Y. C., & Doyle, M. P. (1999). Efficacy of electrolyzed oxidizing water for inactivating *Escherichia coli* O157:H7, *Salmonella enteritidis*, and *Listeria monocytogenes*. *Applied and Environmental Microbiology, 65*, 4276–4276.

Wu, D., Rasco, B., Vixie, K. R., Ünlü, G., Swanson, B., & Liu, Y. (2013). Using Fourier transform infrared (FT-IR) spectroscopy to detect sublethally- or lethally-stressed *Listeria innocua* treated with acetic acid. *LWT - Food Science and Technology, 54*, 456–462.

Yang, H. (2014). *Atomic force microscopy (AFM): Principles, modes of operation and limitations*. Hauppauge, N.Y., USA: Nova Science Publishers, Inc.

Yang, H., Feirtag, J., & Diez-Gonzalez, F. (2013). Sanitizing effectiveness of commercial "active water" technologies on *Escherichia coli* O157:H7, *Salmonella enterica* and *Listeria monocytogenes*. *Food Control, 33*, 232–238.

Ye, Y., Zhang, L., Hao, F., Zhang, J., Wang, Y., & Tang, H. (2012). Global metabolomic responses of *Escherichia coli* to heat stress. *Journal of Proteome Research, 11*, 2559–2566.

Yu, X., & Yang, H. (2017). Pyrethroid residue determination in organic and conventional vegetables using liquid-solid extraction coupled with magnetic solid phase extraction based on polystyrene-coated magnetic nanoparticles. *Food Chemistry, 217*, 303–310.

Zhang, J., & Yang, H. (2017). Effects of potential organic compatible sanitisers on organic and conventional fresh-cut lettuce (*Lactuca sativa* Var. *Crispa* L). *Food Control, 72*, 20–26.

Zhao, L., Zhang, Y., & Yang, H. (2017). Efficacy of low concentration neutralised electrolysed water and ultrasound combination for inactivating *Escherichia coli* ATCC 25922, *Pichia pastoris* GS115 and *Aureobasidium pullulans* 2012 on stainless steel coupons. *Food Control, 73*, 889–899.